Beyond the relativistic Hartree mean-field approximation: Energy dependent effective mass

Vretenar, Dario; Nikšić, Tamara; Ring, Peter

Beyond the relativistic Hartree mean-field approximation: Energy dependent effective mass

D. Vretenar,[1,2] T. Nikšić,[1,2] and P. Ring[2]
[1]*Physics Department, Faculty of Science, University of Zagreb, 10000 Zagreb, Croatia*
[2]*Physics Department, TU Munich, D-85748 Garching, Germany*
(Received 25 July 2001; published 25 January 2002)

The standard relativistic mean-field model is extended by including dynamical effects that arise in the coupling of single-nucleon motion to collective surface vibrations. A phenomenological scheme, based on a linear ansatz for the energy dependence of the scalar and vector components of the nucleon self-energy for states close to the Fermi surface, allows a simultaneous description of binding energies, radii, deformations, and single-nucleon spectra in a self-consistent relativistic framework. The model is applied to the spherical doubly closed-shell nuclei ^{132}Sn and ^{208}Pb.

DOI: 10.1103/PhysRevC.65.024321 PACS number(s): 21.60.Ev, 21.60.Jz, 24.30.Cz

I. INTRODUCTION

Relativistic models based on quantum hadrodynamics [1] provide a microscopic self-consistent description of the nuclear many-body problem. Detailed properties of finite nuclei along the β-stability line have been described with nuclear structure models based on the relativistic mean-field (RMF) approximation [2]. With the unified Dirac-Hartree-Bogoliubov description of mean-field and pairing correlations, the relativistic framework has been very successfully extended to studies of exotic nuclei far from the valley of β stability and to the physics of the drip lines [3–8].

In this framework the single-nucleon dynamics is described by classical equations of motion which are derived self-consistently from a fully relativistic Lagrangian. Standard relativistic nuclear structure models are based on the static approximation, i.e., the nucleon self-energy is real, local and energy independent. Consequently, these models describe correctly the ground-state properties and the sequence of single-particle levels in finite nuclei, but not the level density around the Fermi surface.

In a nonrelativistic mean-field approximation, the total effective mass m^* of a nucleon in a nucleus characterizes the energy dependence of an effective local potential that is equivalent to the, generally nonlocal and frequency dependent, microscopic nuclear potential [9,10]. The total effective mass is a product of the *k* mass which characterizes the nonlocality, i.e., momentum dependence of the mass operator, and the *E* mass which describes the explicit energy dependence of the mass operator. The coupling of single-nucleon motion to collective vibrations and the resulting enhancement of the effective mass around the Fermi surface has been extensively studied in the framework of non-relativistic Hartree-Fock models. For a review, see Refs. [9,10]

In the context of the present analysis, two nonrelativistic microscopic descriptions of the energy dependent effective mass are of particular interest. The analyses of the neutron-^{208}Pb [11], proton-^{208}Pb [12], and neutron-^{40}Ca [13] mean fields were based on dispersion relations that connect the real and imaginary parts of the optical-model potential. The parameters of the complex mean field were determined from available experimental cross sections, and the resulting optical-model potential was extrapolated towards negative energies. A very good agreement was found with the experimental single-particle energies of the valence particle and hole states. In Refs. [14–16] the effects of the collective modes on the single-particle states and the effective mass in ^{208}Pb were calculated in a self-consistent microscopic particle-vibration coupling model. It was shown that, as a function of energy and radial coordinate, the effective mass is enhanced around the Fermi level and on the surface of the nucleus. A similar approach was used in a very recent calculation of the nucleon *E* mass for a medium-heavy deformed nucleus as a function of the rotational frequency along the yrast line [17].

In the relativistic framework, the concept of effective nucleon mass in symmetric nuclear matter and finite nuclei was analyzed by Jaminon and Mahaux in Refs. [18,19]. In addition to the *k* mass and *E* mass, a third effective mass, the ''Lorentz mass'' appears in the relativistic approach. It results from different Lorentz transformation properties of the scalar and vector potentials. In Ref. [19] a quantitative analysis of the energy dependence of the effective mass was performed in the framework of the relativistic Brueckner-Hartree-Fock approximation to the mean field in symmetric nuclear matter. The calculation was based on dispersion relations that connect the imaginary to the real part of the Lorentz components of the mean field. Although in finite nuclei the mechanism which leads to the energy dependence of the effective mass is different, i.e., it results from the coupling of single-nucleon motion to the collective modes, a very useful result of Ref. [19] is that the energy dependence of the total dispersive contribution to the real part of the mean field is almost linear in the region $E_F-10<E<E_F+10$ MeV around the Fermi energy E_F.

In the present work we propose a phenomenological scheme to include the effect of coupling of single-nucleon motion to surface vibrations, i.e., the energy dependence of the nucleon self-energy, in self-consistent relativistic mean field calculations. Rather than calculating the first-order correction to the RMF single-nucleon energy spectra, a linear energy dependence of the scalar and vector potentials is explicitly included in the Dirac equation. The resulting generalized eigenvalue problem can be solved exactly, and this approach gives the possibility to reproduce, in a self-consistent calculation, both the total binding energy and the

density of single-nucleon states around the Fermi surface. The principal advantage over perturbation calculations is, however, that the present approach can be easily extended to constrained calculations in deformed nuclei. The main purpose will be the study of shape coexistence phenomena in chains of isotopes far from the valley of β stability.

II. THE RELATIVISTIC MEAN-FIELD MODEL WITH ENERGY DEPENDENT POTENTIALS

In the framework of the relativistic mean field approximation nucleons are described as point particles that move independently in mean fields which originate from the nucleon-nucleon interaction. The theory is fully Lorentz invariant. Conditions of causality and Lorentz invariance impose that the interaction is mediated by the exchange of pointlike effective mesons, which couple to the nucleons at local vertices. The single-nucleon dynamics is described by the Dirac equation

$$\left\{-i\boldsymbol{\alpha}\cdot\boldsymbol{\nabla}+\beta(m+g_\sigma\sigma)+g_\omega\omega^0+g_\rho\tau_3\rho_3^0+e\frac{(1-\tau_3)}{2}A^0\right\}\psi_i = \varepsilon_i\psi_i . \quad (1)$$

σ, ω, and ρ are the meson fields, and A denotes the electromagnetic potential. g_σ, g_ω, and g_ρ are the corresponding coupling constants for the mesons to the nucleon. The lowest order of the quantum field theory is the mean-field approximation: the meson field operators are replaced by their expectation values. The sources of the meson fields are defined by the nucleon densities and currents. The ground state of a nucleus is described by the stationary self-consistent solution of the coupled system of the Dirac (1) and Klein-Gordon equations

$$[-\Delta+m_\sigma^2]\sigma(\mathbf{r})=-g_\sigma\rho_s(\mathbf{r})-g_2\sigma^2(\mathbf{r})-g_3\sigma^3(\mathbf{r}), \quad (2)$$

$$[-\Delta+m_\omega^2]\omega^0(\mathbf{r})=g_\omega\rho_v(\mathbf{r}), \quad (3)$$

$$[-\Delta+m_\rho^2]\rho^0(\mathbf{r})=g_\rho\rho_3(\mathbf{r}), \quad (4)$$

$$-\Delta A^0(\mathbf{r})=e\rho_p(\mathbf{r}), \quad (5)$$

for the sigma meson, omega meson, rho meson, and photon field, respectively. Due to charge conservation, only the third component of the isovector $\vec{\boldsymbol{\rho}}$ meson contributes. The source terms in Eqs. (2)–(5) are sums of bilinear products of baryon amplitudes, and they are calculated in the no-sea approximation, i.e., the Dirac sea of negative energy states does not contribute to the nucleon densities and currents. Due to time reversal invariance, there are no currents in the static solution for an even-even system, and therefore the spatial vector components $\boldsymbol{\omega}$, $\boldsymbol{\rho}_3$, and $\mathbf{A}$ of the vector meson fields vanish. The quartic potential

$$U(\sigma)=\frac{1}{2}m_\sigma^2\sigma^2+\frac{1}{3}g_2\sigma^3+\frac{1}{4}g_3\sigma^4 \quad (6)$$

introduces an effective density dependence. The nonlinear self-interaction of the σ field is essential for a quantitative description of properties of finite nuclei.

The details of the calculated ground-state properties depend on the choice of the effective Lagrangian. Several effective interactions, i.e., parameter sets of the mean-field Lagrangian have been derived that provide a satisfactory description of nuclear properties along the β-stability line. In particular, the parameter set NL3 [20,21] has been adjusted to ground state properties of a large number of spherical nuclei. Properties calculated with the NL3 effective interaction are found to be in very good agreement with experimental data for spherical and deformed nuclei at and away from the line of β stability. In particular, NL3 has been used in most applications of the relativistic Hartree-Bogoliubov model to the physics of drip-line nuclei [3–8].

The effective potential that determines the ground state of a finite nucleus is essentially given by the sum of the scalar σ potential (attractive) and the vector ω potential (repulsive). Both potentials are of the order of several hundred MeV in the nuclear interior. The contributions of the isovector ρ-meson field and the electromagnetic interaction are, of course, much smaller. In the relativistic Hartree mean-field approximation the nucleon self-energy is real, local, and energy independent. It should be emphasized, however, that even in the Hartree approximation the equivalent Schrödinger potential is nonlocal, i.e., momentum dependent. This results from the momentum dependence of the scalar density, or equivalently, the momentum dependence of the Dirac mass in the nonrelativistic reduction of the Dirac equation.

A phenomenological description of the effect of coupling between single-nucleon motion and collective modes can be obtained by assuming that the scalar and vector potentials depend linearly on energy in the vicinity of the Fermi surface

$$V_\sigma(r,E)=V_\sigma(r)+\alpha(E-E_F),$$

$$V_\omega(r,E)=V_\omega(r)+\alpha(E-E_F), \quad (7)$$

where $V_\sigma(r)$ and $V_\omega(r)$ denote the usual, energy independent potentials. For simplicity, we only consider the energy dependence of the two most important contributions to the effective potential, i.e., the σ and ω fields. As we have already emphasized in the Introduction, in their analysis of the Fermi surface anomaly and depletion of the Fermi sea in the relativistic Brueckner-Hartree-Fock approximation [19], Jaminon and Mahaux have shown that the total dispersive contribution to the real part of the mean field potential displays an almost linear energy dependence in a region of $\approx\pm10$ MeV around the Fermi energy. A linear energy dependence of the real part of the mean field potential in the region $E_F-5<E<E_F+5$ was also found in the calculation of the nucleon effective mass in ^{208}Pb in the framework of the microscopic particle-vibration coupling model (see Fig. 1 of Ref. [16]). If the effective potential in the Dirac equation depends only linearly on energy, this defines a generalized eigenvalue problem

$$H_D|\psi\rangle=AE|\psi\rangle, \quad (8)$$

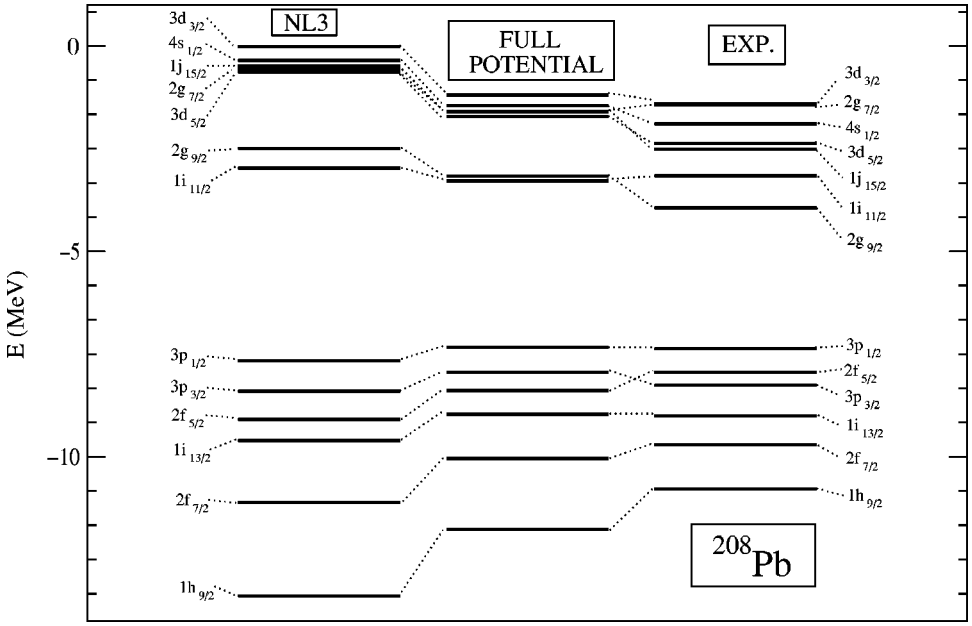

FIG. 1. Neutron single-particle states in ^{208}Pb. In the first column on the left the relativistic Hartree mean-field results calculated with the NL3 effective interaction are displayed, the levels calculated with the energy dependent effective potential are shown in the second column, and the right-hand column gives the experimental spectrum [26,27].

where H_D is the energy independent Dirac Hamiltonian [see Eq. (1)], and on the right-hand side $A\times E$ is the matrix which contains the linear energy dependence. Equation (8) can be solved exactly, and in this way the effect of coupling to collective modes can be included in the self-consistent calculation of the ground state of a nucleus.

In principle, there is no deeper reason for the σ and ω potentials to have the same energy dependence. If they have, like in Eqs. (7), the total correction to the effective single-nucleon potential is $2\alpha(E-E_F)$, and there is no correction to the spin-orbit term of the effective potential, which is given by the difference of the σ and ω potentials [2]. Since in the present analysis we are only interested in the effect on the density of states around the Fermi level, we assume the same linear energy dependence for V_σ and V_ω. This means that, in principle, an additional parameter can be adjusted to obtain, if necessary, a better agreement for the energy splittings of the spin-orbit partner levels in spherical or deformed nuclei.

The ground state of a spherical or deformed nucleus is obtained from a self-consistent solution of the coupled system of equations: the Dirac generalized eigenvalue equation (8), and the Klein-Gordon equations (2)–(5). The equations are solved by expanding the nucleon spinors and the meson fields in a spherical or deformed harmonic oscillator basis. In the present work we only consider spherical nuclei. Instead of calculating an energy dependent correction to single nucleon spectra determined by some of the standard RMF parameter sets such as NL3, we include the energy dependent potentials in the fitting procedure that is used to construct an effective interaction. By adjusting the meson-nucleon coupling constants, the mass of the σ meson, the parameters of the σ meson self-interaction terms, and the parameter α of the linear energy dependence in Eqs. (7), to nuclear matter and properties of finite spherical nuclei, we seek to obtain a simultaneous description of binding energies and of densities of single-nucleon states in the valence shells.

In order to illustrate the method, in the present analysis we calculate the single-nucleon spectra of the doubly closed-shell nuclei ^{208}Pb and ^{132}Sn. In this particular calculation the starting point is the NL3 parameter set. This effective interaction has been adjusted to ground-state properties of a number of spherical nuclei and, of course, it reproduces the binding energies of ^{208}Pb and ^{132}Sn. The calculated densities of single-nucleon states around the Fermi surface are, however, too low as compared with the experimental spectra, i.e., the effective mass is too low and energy independent. By including the linear energy dependence (7) in the effective single-nucleon potential of the Dirac equation, the binding is obviously reduced and the parameter set of the effective interaction has to be readjusted. In principle, the parameter of the energy dependence α in Eqs. (7) can be calculated from the imaginary part of the optical potential by using dispersion relations, or by coupling single-nucleon states to core vibrations calculated with the relativistic random phase approximation. That would, of course, mean a different α for every nucleus. In the present self-consistent method α is an adjustable parameter, determined by a fit to ground state properties, together with the parameter set of the effective Lagrangian. In this work we only calculate ^{208}Pb and ^{132}Sn, although of course a larger set of nuclei would be necessary to obtain an optimal set of parameters. For closed-shell nuclei without pairing, the Fermi energy is taken as the half-energy between the last occupied and the first unoccupied single-nucleon orbit. The linear energy correction to the effective potential is confined to the window $E_F-10<E<E_F+10$ MeV. In addition to the available binding energies and radii, the fitting procedure is constrained with the average energies of hole and particle states in the last occupied and the first unoccupied major shells, respectively.

In each iteration step, and for given single-nucleon angular momentum and parity, the generalized eigenvalue problem (8) is solved in two steps. In the first step the single-nucleon energy independent Dirac Hamiltonian H_D [see Eq. (1)] is diagonalized in the harmonic oscillator basis. From the resulting single-nucleon spectrum we determine the

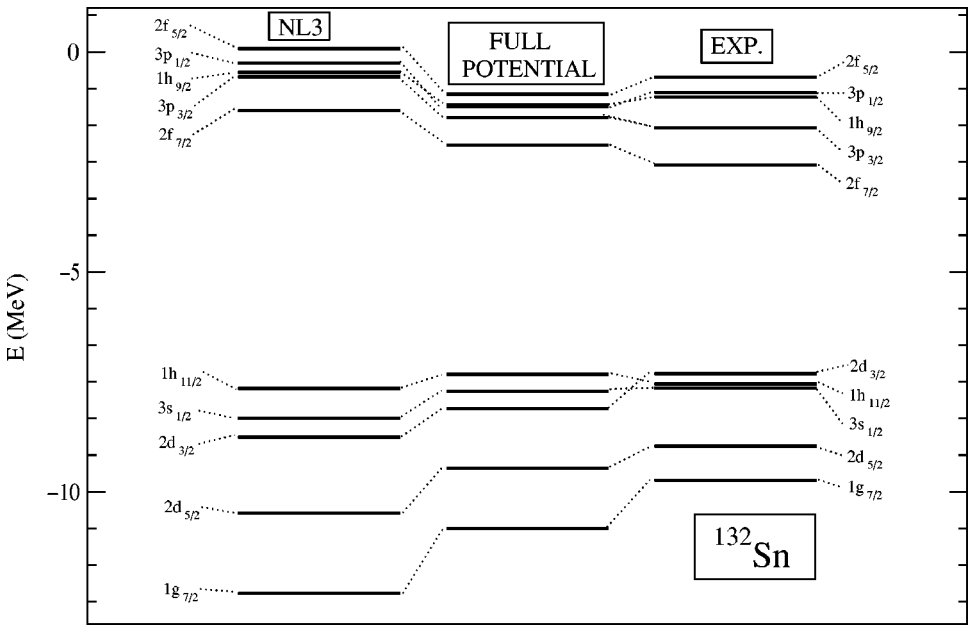

FIG. 2. Same as in Fig. 1, but for the neutron single-particle states in ^{132}Sn. The experimental data are from Refs. [22–25].

eigenvectors ψ_i with eigenvalues ϵ_i in the energy interval $\approx\pm 10$ MeV around the Fermi energy. In the next step the matrix of the generalized eigenvalue problem is constructed

$$H_{ij}=\begin{cases}\langle\psi_i|H_D|\psi_j\rangle, \\ \langle\psi_i|H_D+2\alpha(E-E_f)|\psi_j\rangle \\ \text{for } E_F-10<\epsilon_i,\epsilon_j<E_F+10 \text{ MeV}.\end{cases} \tag{9}$$

For a solution in coordinate space, the equivalent of this two-step procedure is the inclusion of the theta function $\Theta(10 \text{ MeV}-|E-E_F|)$ in front of the energy dependent correction in Eq. (7). Although we do not include an explicit radial dependence for the second term in Eq. (7), its contribution obviously vanishes at large distances, i.e., all matrix elements H_{ij} vanish for large r because $\psi_i(\vec{r})\rightarrow 0$.

The set of states which is the solution of the generalized eigenvalue problem is not orthogonal. This is not a big effect, however, because the energy dependent correction to the potential is relatively small, and it affects only a small number of states in the vicinity of the Fermi level. After the orthogonalization, the new set of orthonormalized states is identified with the single-nucleon spectrum. There is no significant difference between the diagonal matrix elements of the Hamiltonian in this basis, i.e., the ''single-particle energies,'' and the original eigenvalues. We have verified that the same value for the ground-state energy is obtained when this quantity is calculated as the sum of kinetic and potential energies, or as the sum of the ''single-nucleon energies'' and the energies of the meson fields.

The resulting single-neutron spectra in ^{208}Pb and ^{132}Sn are displayed in Figs. 1 and 2, respectively. they are compared with the relativistic Hartree mean-field results calculated with the NL3 interaction, and with experimental single-neutron spectra [22–27]. In comparison with the original NL3 interaction, we note a considerable improvement of the calculated spectra. The increase of the density of states around the Fermi surface results from the energy dependence of the effective mass. The spectra obtained with the full potential are in good agreement with the experimental single-neutron levels. The energy dependent correction, however, seldom changes the ordering of states, and therefore we still find inverted doublets, such as, for example, $2f_{5/2}$-$3p_{3/2}$ and $1i_{11/2}$-$2g_{9/2}$ in ^{208}Pb. In Table I we compare the NL3 effective interaction with the new set of parameters which is obtained by including the energy dependent correction to the single-nucleon potential in the fitting procedure. We note that the values of the parameters change very little as compared with the original NL3 parametrization, with the exception of a somewhat more pronounced decrease of the rho-meson coupling. The adjusted value of the coefficient of the linear energy dependence in Eqs. (7) is $2\alpha=-0.288$. This value can be compared with the one calculated in the self-consistent microscopic particle-vibration coupling model of Refs. [14–16]. For proton states $E_F-5<E<E_F+5$ MeV in ^{208}Pb (see Fig. 1 of Ref. [16]), the coefficient of linear energy dependence of the real part of the mass operator is

TABLE I. The parameter set of the NL3 effective interaction [21] (center column), and the new interaction (right column) which results from the inclusion of the linear energy dependence in the effective single-nucleon potential.

	NL3	NEW
m	939.0 MeV	939.0 MeV
m_σ	508.1941 MeV	508.8500 MeV
m_ω	782.5010 MeV	782.5550 MeV
m_ρ	763.0 MeV	763.0 MeV
g_σ	10.2169	10.2200
g_ω	12.8675	12.8730
g_ρ	4.4744	4.4000
g_2	-10.4307 fm^{-1}	-10.2153 fm^{-1}
g_3	-28.8851	-29.0960
2α		-0.288

≈ -0.35. In addition to single-nucleon spectra, we also compare the experimental and calculated binding energies: for ^{208}Pb the experimental value is -1636.47 MeV, the value calculated with NL3 is -1639.54 MeV, and the full, energy dependent effective potential gives -1636.80 MeV. For ^{132}Sn, the binding energy calculated with NL3 is -1105.44 MeV, the value obtained with the new parameter set is -1101.31 MeV, and the experimental binding energy is -1102.90 MeV.

The single-neutron spectrum of ^{208}Pb can be compared with those obtained with the self-consistent microscopic particle-vibration coupling model (see Fig. 2 of Ref. [15]), and with the phenomenological dispersion relation analysis of Ref. [11] (see Fig. 9 of that article). In comparison with the experimental spectrum, the results of the present calculation are somewhat better than those obtained with the microscopic particle-vibration coupling, but not as good as the spectrum which results from dispersion relations between the real and imaginary parts of the optical-model potential. This is, of course, not very surprising. In the analysis of Ref. [15] the mass operator is the sum of a Hartree-Fock term and an energy dependent term which arises from the coupling to the microscopically calculated RPA vibrations. A number of approximations have to be made in such a microscopic calculation, which will necessarily affect the quality of the final single-nucleon spectrum. On the other hand, there is no adjustable parameter such as α in the microscopic calculation. In the phenomenological analysis of Ref. [11] the total dispersive contribution to the effective potential is written as a sum of volume and surface components. A relatively large number of parameters was used to adjust these two contributions separately. It was shown that about 40% of the total correction results from volume dispersive effects and about 60% from the surface-peaked correction. The comparison with the single-neutron spectra of Refs. [15,11], as well as with the experimental data, shows that our linear ansatz (7) presents a very good approximation of the dynamical effects which arise from the coupling of single-nucleon and collective degrees of freedom.

In Tables II and III we list both the neutron and the proton levels of ^{208}Pb and ^{132}Sn, respectively. For the last occupied and first unoccupied major shells, we compare the results calculated with the standard relativistic Hartree mean-field approximation (NL3 interaction), the energy spectrum calculated with the full, energy dependent model potential, and the experimental energies. In addition, we compare the average energies of hole (particle) states

$$\langle E \rangle = \frac{\sum_{nlj} (2j+1) E_{nlj}}{\sum_{nlj} (2j+1)}, \tag{10}$$

where the sum runs over occupied (unoccupied) states within a major shell. Obviously the inclusion of linear energy dependence in the nucleon self-energy considerably improves the calculated single-nucleon spectra, while at the same time it enables the self-consistent calculation of global ground state properties, such as the binding energy and radii.

TABLE II. Neutron (left panel) and proton (right panel) single-particle energies E_{nlj} in ^{208}Pb. For each panel, the left-hand column specifies the radial, orbital, and total angular momentum quantum numbers, the column labeled NL3 contains results calculated with the standard relativistic Hartree mean-field approximation, the energy spectrum calculated with the full, energy dependent, model potential is displayed in the third column. Theoretical spectra are compared to the experimental energies shown in the column labeled EXP. With boldface letters are listed the average energies for particle and hole states.

	Neutron state				Proton state		
nlj	NL3	Full	Exp	nlj	NL3	Full	Exp
$4s_{1/2}$	-0.36	-1.46	-1.90	$3p_{1/2}$	2.58	0.60	-0.17
$3d_{3/2}$	-0.02	-1.19	-1.40	$3p_{3/2}$	1.83	0.00	-0.68
$3d_{5/2}$	-0.63	-1.72	-2.37	$2f_{5/2}$	0.55	-0.92	-0.98
$2g_{7/2}$	-0.57	-1.60	-1.44	$2f_{7/2}$	-1.44	-2.55	-2.90
$2g_{9/2}$	-2.50	-3.17	-3.94	$1h_{9/2}$	-4.60	-4.97	-3.80
$1i_{11/2}$	-2.97	-3.29	-3.16	$1i_{13/2}$	-1.03	-2.37	-2.19
$1j_{15/2}$	-0.48	-1.60	-2.51	$\boldsymbol{E_p}$	**-1.28**	**-2.45**	**-1.79**
$\boldsymbol{E_p}$	**-1.33**	**-2.20**	**-2.63**				
$3p_{1/2}$	-7.67	-7.34	-7.37	$3s_{1/2}$	-8.15	-7.95	-8.01
$3p_{3/2}$	-8.41	-7.94	-8.26	$2d_{3/2}$	-9.25	-8.79	-8.36
$2f_{5/2}$	-9.09	-8.38	-7.94	$2d_{5/2}$	-10.88	-10.16	-9.68
$2f_{7/2}$	-11.11	-10.05	-9.71	$1g_{7/2}$	-15.05	-13.55	-11.48
$1h_{9/2}$	-13.39	-11.78	-10.78	$1h_{11/2}$	-10.21	-9.82	-9.35
$1i_{13/2}$	-9.60	-8.97	-9.00	$\boldsymbol{E_h}$	**-11.30**	**-10.57**	**-9.38**
$\boldsymbol{E_h}$	**-10.47**	**-9.55**	**-9.25**				

III. CONCLUSIONS

In applications of standard relativistic mean-field models to the description of ground state properties of spherical and deformed nuclei, the nucleon self-energy is real, local, and energy independent. This leads to the well known problem of low effective mass, i.e., low density of single-nucleon states close to the Fermi surface. In the nonrelativistic framework, this problem has been considered in first-order perturbation,

TABLE III. Same as in Table II, but for the neutron and proton single-particle states in ^{132}Sn.

	Neutron state				Proton state		
nlj	NL3	Full	Exp	nlj	NL3	Full	Exp
$2f_{5/2}$	0.08	-0.96	-0.58	$3s_{1/2}$	-4.22	-6.27	-6.83
$3p_{1/2}$	-0.26	-1.25	-0.92	$1h_{11/2}$	-5.33	-7.33	-6.84
$1h_{9/2}$	-0.46	-1.21	-1.02	$2d_{3/2}$	-5.29	-7.08	-7.19
$3p_{3/2}$	-0.57	-1.50	-1.73	$2d_{5/2}$	-7.05	-8.56	-8.67
$2f_{7/2}$	-1.33	-2.12	-2.58	$1g_{7/2}$	-9.95	-10.77	-9.63
$\boldsymbol{E_p}$	**-0.59**	**-1.44**	**-1.03**	$\boldsymbol{E_p}$	**-6.73**	**-8.32**	**-7.92**
$2d_{3/2}$	-8.76	-8.03	-7.31	$1g_{9/2}$	-16.12	-16.06	-15.71
$1h_{11/2}$	-7.65	-7.33	-7.55	$2p_{1/2}$	-17.11	-16.65	-16.07
$3s_{1/2}$	-8.33	-7.71	-7.64	$\boldsymbol{E_h}$	**-16.28**	**-16.15**	**-15.77**
$2d_{5/2}$	-10.48	-9.47	-8.96				
$1g_{7/2}$	-12.31	-10.84	-9.74				
$\boldsymbol{E_h}$	**-10.65**	**-9.55**	**-8.81**				

either by explicitly coupling the single-nucleon states to collective RPA modes, or by using dispersion relations that connect the real and imaginary parts of the optical-model potential. In the present work we have studied a phenomenological scheme which allows the inclusion of the dynamical effects of coupling of single-nucleon motion to surface vibrations in self-consistent relativistic mean field calculations. The scheme is based on a linear ansatz for the energy dependence of the scalar and vector components of the nucleon self-energy for states close to the Fermi surface. This defines a generalized Dirac eigenvalue problem, which can be solved self-consistently together with the Klein-Gordon equations for the meson fields. Thus, rather than calculating the first-order correction to the single-nucleon spectra, the assumption of linear energy dependence for the mass operator enables a self-consistent calculation of both the global ground state properties (masses, radii) and the single-nucleon levels around the Fermi surface. The model that we have studied might be especially useful in studies of shape-coexistence phenomena in nuclei far from the valley of β stability. Because of the simple linear energy dependence of the effective single-nucleon potential, the method can be easily extended to constrained calculations in deformed nuclei.

In the present work the method has been tested on the spherical, doubly closed-shell nuclei ^{132}Sn and ^{208}Pb. The ground-state properties of these nuclei are well described by the standard NL3 effective interaction of the relativistic mean-field model. With the inclusion of linear energy dependent terms in the scalar and vector components of the nucleon self-energy for states close to the Fermi surface, the parameter set of the effective Lagrangian has to be readjusted in order to reproduce both the global ground state properties and the densities of single-nucleon states. The resulting single-nucleon spectra have been compared with experimental data, as well as with previous nonrelativistic first-order perturbation calculations for ^{208}Pb. It has been shown that the energy dependent effective mass considerably improves the calculated single-nucleon spectra. By allowing the simultaneous description of binding energies, radii and single-nucleon spectra, the self-consistent method studied in this work presents a natural phenomenological extension of the relativistic mean-field model. Work is in progress on the derivation of the energy dependent effective mass by coupling single-nucleon states to surface vibrations calculated in the relativistic random phase approximation, and on the extension of the model to deformed nuclei.

ACKNOWLEDGMENTS

This work was supported in part by the Bundesministerium für Bildung und Forschung under Project No. 06 TM 979. D.V. and T.N. would like to acknowledge the support from the Alexander von Humboldt-Stiftung.

[1] B.D. Serot and J.D. Walecka, Adv. Nucl. Phys. **16**, 1 (1986); Int. J. Mod. Phys. E **6**, 515 (1997).
[2] P. Ring, Prog. Part. Nucl. Phys. **37**, 193 (1996).
[3] W. Pöschl, D. Vretenar, G.A. Lalazissis, and P. Ring, Phys. Rev. Lett. **79**, 3841 (1997).
[4] G.A. Lalazissis, D. Vretenar, W. Pöschl, and P. Ring, Nucl. Phys. **A632**, 363 (1998).
[5] G.A. Lalazissis, D. Vretenar, P. Ring, M. Stoitsov, and L. Robledo, Phys. Rev. C **60**, 014310 (1999).
[6] D. Vretenar, G.A. Lalazissis, and P. Ring, Phys. Rev. Lett. **82**, 4595 (1997).
[7] G.A. Lalazissis, D. Vretenar, and P. Ring, Nucl. Phys. **A650**, 133 (1999).
[8] G.A. Lalazissis, D. Vretenar, and P. Ring, Phys. Rev. C **63**, 034305 (2001).
[9] C. Mahaux, P. F. Bortignon, R. A. Broglia, and C. H. Dasso, Phys. Rep. **120**, 1 (1985).
[10] C. Mahaux and R. Sartor, Adv. Nucl. Phys. **20**, 1 (1996).
[11] C. H. Johnson, D. J. Horen, and C. Mahaux, Phys. Rev. C **36**, 2252 (1987).
[12] C. Mahaux and R. Sartor, Nucl. Phys. **A503**, 525 (1989).
[13] C. H. Johnson and C. Mahaux, Phys. Rev. C **38**, 2589 (1988).
[14] V. Bernard and Nguyen van Giai, Nucl. Phys. **A327**, 397 (1979).
[15] V. Bernard and Nguyen van Giai, Nucl. Phys. **A348**, 75 (1980).
[16] Nguyen Van Giai and Pham Van Thieu, Phys. Lett. **126B**, 241 (1983).
[17] P. Donati, T. Dossing, Y. R. Shimizu, S. Mizutori, P. F. Bortignon, and R. A. Broglia, Phys. Rev. Lett. **84**, 4317 (2000).
[18] M. Jaminon and C. Mahaux, Phys. Rev. C **40**, 354 (1989).
[19] M. Jaminon and C. Mahaux, Phys. Rev. C **41**, 697 (1990).
[20] B. ter Haar and R. Malfliet, Phys. Rep. **149**, 207 (1987).
[21] G.A. Lalazissis, J. König, and P. Ring, Phys. Rev. C **55**, 540 (1997).
[22] P. Hoff *et al.*, Phys. Rev. Lett. **77**, 1020 (1996).
[23] M. Sanchez-Vega, B. Fogelberg, H. Mach, R.B.E. Taylor, and A. Lindroth, Phys. Rev. Lett. **80**, 5504 (1998).
[24] T. Bjornstad *et al.*, Nucl. Phys. **A453**, 463 (1986).
[25] G.A. Stone, S.H. Faller, and W. Walters, Phys. Rev. C **39**, 1963 (1989).
[26] M.J. Martin, Nucl. Data Sheets **63**, 723 (1991).
[27] M.J. Martin, Nucl. Data Sheets **70**, 315 (1993).